

# Strategic Optimization and Application Analysis of Orthogonal Frequency Division Multiplexing Index Modulation Systems

Haochen Liao

School of Information and Communication Engineering, University of Electronic Science and Technology of China Chengdu, 611731, China

\* Corresponding Author Email: 1811421133@mail.sit.edu.cn

**Abstract.** Orthogonal Frequency Division Multiplexing (OFDM) is a type of Multi-Carrier Modulation that operates by dividing a single channel into numerous orthogonal subchannels. By doing this, it facilitates the transformation of high-speed digital signals into parallel subdata streams. These streams are then modulated onto the subchannels, thereby enabling efficient transmission. OFDM with Index Modulation (OFDM-IM) further enhances this process by combining the benefits of OFDM with the high spectral efficiency of spatial modulation techniques, leading to significant improvements in the bit-error rate performance of the system. Despite the advantages of OFDM-IM systems, several challenges exist. For instance, the presence of inconsistent sampling rates can result in amplitude distortion. Furthermore, a high peak-to-average power ratio can adversely impact the efficiency of the RF power amplifier. These problems necessitate the exploration of diverse solutions to improve the performance of OFDM-IM systems. The focus of this thesis is to investigate and assess different strategies aimed at addressing these issues within OFDM-IM systems. We will explore these strategies, compare their effectiveness, and offer comprehensive recommendations on their optimal applications based on specific system requirements and scenarios. In doing so, the goal is to pave the way for more effective and efficient implementation of OFDM-IM systems in diverse contexts.

**Keywords:** OFDM-IM, Permutation mode, ML detection.

## 1. Introduction

The first optimization scheme is Permutation Mode OFDM-IM (PM-OFDM-IM), which introduces the subcarrier index arrangement mode to transmit additional data information by separating the data of the sub-block at the transmitting end and employing different constellation point mappings [1]. Simulation results of the achievable bit rate (ABR) demonstrate that PM-OFDM-IM effectively improves subcarrier utilization. When compared to other optimization schemes, PM-OFDM-IM exhibits favorable resistance to frequency offset while achieving similar subcarrier utilization, as well as superior bit error performance in both Gaussian and Rayleigh channels.

The core principle of PM-OFDM-IM revolves around introducing permutation information through permutation-activated subcarriers to enhance subcarrier utilization. The arrangement pattern is achieved by mapping distinguishable constellation symbols onto the activated subcarriers [2]. As illustrated in the accompanying figure (Figure 1), the P bit is divided into two parts: P1 bits represent extra information bits, while P2 bits undergo normal constellation mapping. P1 bits comprise index selection bits (P1I) and arrangement selection bits (P1S). The index selection bits activate specific subcarriers for each subblock, while the arrangement selection bits determine the arrangement of the activated subcarriers. The transmission bit P2 is divided into J parts and enters different mapping modules. In comparison to the OFDM-IM system, the PM-OFDM-IM system is equipped with an arrangement and selection module, enabling the transmission of arrangement selection bits [3].

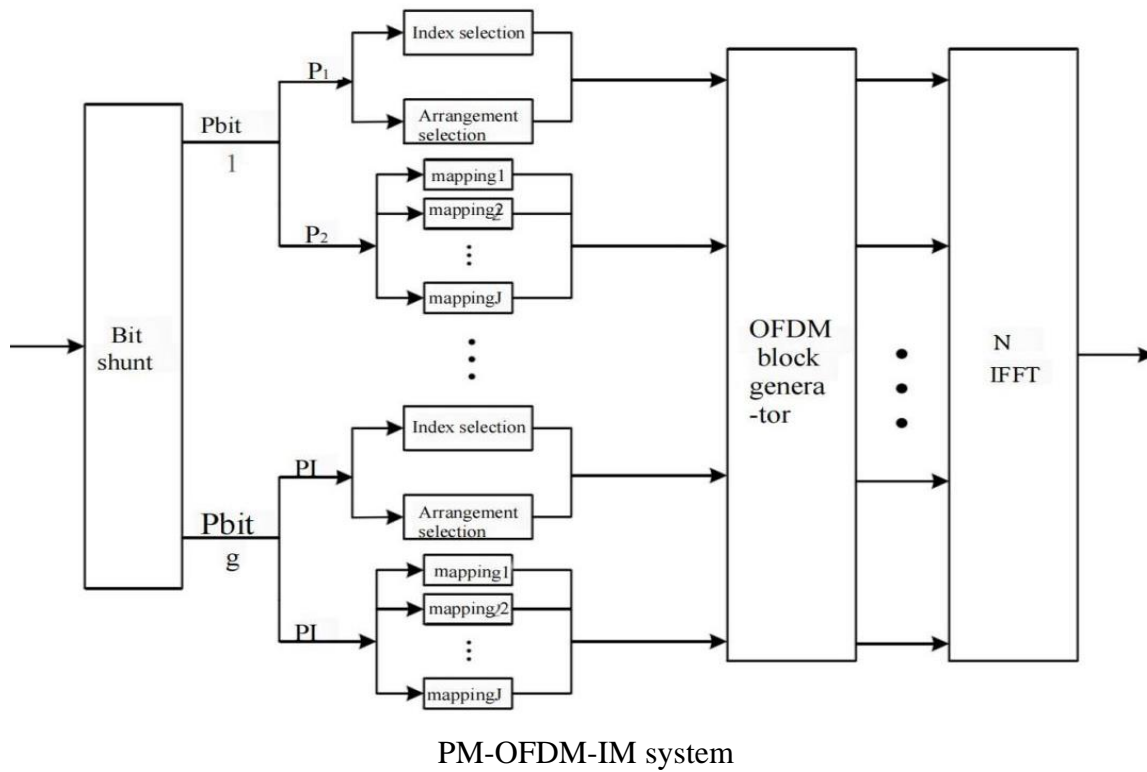


**Fig. 1** In an L-J PM-OFDM-IM system, there are L subcarriers in the subblock, activate J of them, according to the formula, the number of index bits of the subblock is.

$$P_{1l} = \lceil \log_2 C_L^J \rceil \tag{1}$$

Arrange the activated subcarriers, according to the permutation combination formula, J different mapping modes can be arranged, and the number of arrange selection bit is

$$P_{1s} = \lceil \log_2 J! \rceil \tag{2}$$

Therefore, the total number of bits of extra information is

$$P_1 = \lceil \log_2 C_L^J \rceil + \lceil \log_2 J! \rceil \tag{3}$$

If the modulation order of the constellation on the ith activator carrier is  $iM$ , where  $i=1, 2, \dots, J$ . Transmission bit  $2P$  can be expressed as

$$P_2 = \sum_{i=1}^J \log_2 M_i \tag{4}$$

Then the subcarrier utilization of the PM-OFDM-IM system can be expressed as

$$\eta_{PM-OFDM-IM} = \frac{\lceil \log_2 C_L^J \rceil + \lceil \log_2 J! \rceil + \sum_{i=1}^J \log_2 M_i}{L} \tag{5}$$

Compare to the former formula, it has  $\lceil \log_2 J! \rceil$  and when the J value increases, the subcarrier utilization of the PM-OFDM-IM system will be higher than that of the OFDM-IM system [4].

## 2. The Implementation Method of PM-OFDM-IM

In the PM-OFDM-IM system, additional information includes index information and arrangement information, which controls the position of the active subcarrier and the arrangement of the transmission subcarrier, respectively. Like the OFDM-IM system, PM-OFDM-IM can be realized by two methods: lookup table method and permutation combination method [5].

### 2.1. Lookup Method:

In this method, the sender side of the PM-OFDM-IM system creates and sends a lookup table. Lookup tables are provided.

The corresponding information of index bits, arrangement bits, and subcarrier transmission modes. Demodulate indexing and arranging bit information only.

The opposite needs to be done on the receiving end through the table's information. For example, in a 4-3 PM-OFDM-IM department. In the system, the total number of selections is  $C_4^3=4$ , the total number of permutations is  $3!=6$ , the corresponding index selection is 2 bits, and the permutation bits are 2 bits. Let the symbols of the transmission bits be mapped by different constellations 1Q, 2Q, and 3Q respectively. The correspondence between the sending mode of each subblock and the index bit and the arrangement bit is shown in table below. As can be seen from the table, the index bit controls '0', which is the position of the silent subcarrier. Permutation bits control rows of 1Q, 2Q, 3Q constellation symbols Sequence. At the receiving end, the index and arrangement bits in each table are deactivated by the transmit mode, the index bits and permutation bits are decalled, and finally the transmission bits on the active subcarrier are decalled.

### 2.2. Permutation and Combination Method:

Permutation and combination use mathematical formulas to provide a one-to-one correspondence between natural numbers and each sending mode.

In the L-J PM-OFDM-IM system, the total activation mode of the index bit has  $Z_s$ , satisfying  $Z_s \in [0, C(L, J) - 1]$ , according to the combination formula  $Z_s$  can be split and expressed as

$$Z_s = C_L^J = C(d_j - 1, J) + \dots + C(d_2 - 1, 2) + C(d_1 - 1, 1) \quad (6)$$

where  $D=(d_j, d_{j-1}, \dots, d_1), d_j > d_{j-1} > \dots > d_1$ , expressed as a decreasing sequence mapped by the natural number  $Z_s$ , that is, the sequence of subcarrier positions corresponding to activation. Define  $C(a, a+1)=0$  and  $a$  as an integer. Activated subcarrier arrangement. The total number of modes is  $Z_p$  species, satisfying  $Z_p \in [0, J! - 1]$ . After detection by the receiving end, the arrangement of subcarriers is activated. The sequence is expressed as  $C=(C_j, C_{j-1}, \dots, C_1)$ . Define a  $Q(1, 2, \dots, j)$  to represent the set of natural numbers from 1 to  $j, \varphi_j$

Indicates the seat number of  $c_j$  in  $Q$ . Look for it first  $c_j$  in the seat number in the set  $Q$ , get  $\varphi_j$ , the next step is deleted  $c_j$  in  $Q$ , then find the seat number of  $c_{j-1}$ , which is  $\varphi_{j-1}$  in the new set  $Q$ , and so on until the last seat number of the last element is found.

## 3. PM-OFDM-IM System Performance Analysis

In this chapter, the upper bound of bit error rate of the PM-OFDM-IM system is derived by the parallel boundary analysis method, and the anti-frequency bias ability of PM-OFDM-IM and the attainability of the system derived by mutual information are analyzed.

Upper bounds of bit error rate:

In a PM-OFDM-IM system, each subblock is sent and demodulated separately, and according to the union analysis method, the bit error rate of PM-OFDM-IM can be expressed as

$$P_E = \frac{1}{G} \sum_{g=1}^G P_{e,g} \quad (7)$$

$P_{e,g}$  is the  $g$ th subcarrier block, which can be expressed as

$$P_{e,g} = \frac{1}{P \cdot 2^P} \sum_{X_g} \sum_{\hat{X}_g} P(X_g \rightarrow \hat{X}_g) e(X_g \rightarrow \hat{X}_g) \quad (8)$$

Where  $e(X_g \rightarrow \hat{X}_g)$  is the number of misbits, caused by the misjudgment of the minimum Euclidean distance, and Unconditional pairwise error probability of PM-OFDM-IM system  $P(X_g \rightarrow \hat{X}_g)$  can be expressed as

$$P(X_g \rightarrow \hat{X}_g) \leq \frac{1}{12\det(I_1 + v_1 K_1 A_g)} + \frac{1}{4\det(I_1 + v_2 K_1 A_g)} \quad (9)$$

When the channel conditions are poor, the channel estimation error increases, the values of variables  $v_1$  and  $v_2$  become smaller, and the probability of unconditional pairwise errors increase. In summary, the upper bound of the bit error rate of the PM-OFDM-IM system is mainly related to the channel conditions and the midpoint of the constellation diagram is related to the minimum Euclidean distance between points. Frequency offset resistance: To simplify the calculation, only CFO and Gaussian noise are considered in the channel. As with the OFDM system, the PM-OFDM IM signal passes through the channel and then at the receiving end, and the interference on the  $k$ th subcarrier comes from two parts, ICI and noise, which can be expressed as

$$N_k = I_\alpha(k) + W_\alpha(k) \quad (10)$$

Like the OFDM-IM system, the PM-OFDM-IM system still has a large number of silent subcarriers, thereby reducing the ICI variance. According to Equation, the PPEP OF THE PM-OFDM-IM system is reduced, and the upper bound of the bit error rate obtained by the bounds is reduced, so the PM-OFDM-IM system also has strong resistance to frequency offset [6].

### 3.1. Simulation Analysis

This section simulates PM-OFDM-IM from three aspects, namely BER under Gaussian channel and Rayleigh channel, and BER and ABR that change the frequency offset coefficient. Due to the comparison of different optimization models, in some scenarios subcarrier utilization cannot be consistent, so similar subcarrier utilization rates are used for simulation comparison in this section.

### 3.2. Bit Error Rate Simulation

Firstly, the BER OF PM-OFDM-IM and other index optimization systems under Gaussian channel and Rayleigh channel are simulated and compared. As shown in Table 1 and 2.

**Tab. 1** Gaussian channel PM-OFDM-IM simulation parameter table

<b>Gaussian channel PM-OFDM-IM simulation parameter table</b>	
<b>Parameter</b>	<b>Value</b>
<b>Number of subcarriers</b>	192
<b>Number of iterations</b>	2000
<b>Subcarrier spacing</b>	15kHz

**Tab. 2** Rayleigh channel PM-OFDM-IM simulation parameter table

<b>Rayleigh channel PM-OFDM-IM simulation parameter table</b>	
<b>Parameter</b>	<b>Value</b>
<b>Number of subcarriers</b>	1024
<b>The length of CP</b>	32
<b>Number of iterations</b>	2000
<b>Subcarrier spacing</b>	15kHz
<b>Number of fading paths</b>	10

Since the subcarrier utilization of OFDM is an integer, the OFDM subcarrier utilization is selected as 2bps/Hz. The remaining indexed modulation schemes all use the same subcarrier utilization of

2bps/Hz. In the Rayleigh channel, OFDM and OFDM-IM are 1bps/Hz, and other indexing schemes are 1.33bps/Hz.

As the image below shows, the BER performance of all indexing systems under the Gaussian channel is better than that of the OFDM system. When  $0 \text{Eb/N} \leq 6 \text{ dB}$ , the MM-OFDM-IM system has the best bit error performance. With the gradual increase of  $0 \text{Eb/N}$  value, at  $0 \text{Eb/N} = 10 \text{ dB}$ , OFDM-HIQ-IM has the best bit error performance, followed by PM-OFDM-IM and OFDM-IM.

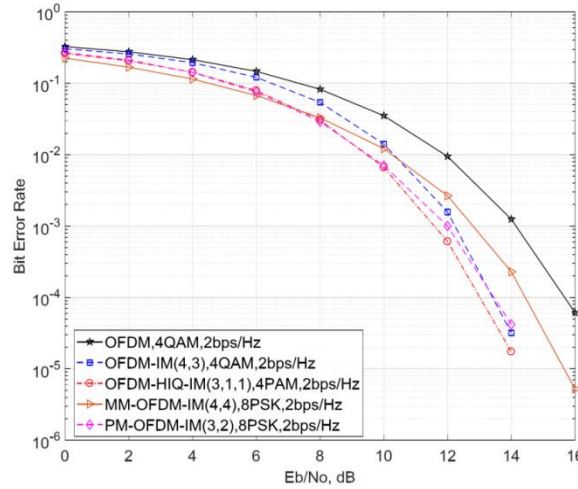


**Fig. 2** Performance Comparison of Different Mapping Schemes Under Rayleigh Channel Conditions

As shown in Figure 2, at  $E_b/N_0 > 10 \text{ dB}$ , all index systems have a lower BER than OFDM systems. Under the low signal-to-noise ratio, the bit error rate curves of OFDM-IM, OFDM-HIQ-IM and PM-OFDM-IM are similar, and the bit error rate curves of OFDM-HIQ-IM and PM-OFDM-IM coincide with each other and have the same bit error rate. When  $E_b/N_0 > 30 \text{ dB}$ , the PM-OFDM-IM index system with 1.33bps/Hz has the best bit error performance, followed by the 1.33bps/Hz OFDM-HIQ-IM system, and the worst indexing scheme is the 1.33bps/Hz MM-OFDM-IM scheme. Since the MM-OFDM-IM subblock activates all subcarriers, resulting in no silent subcarrier during transmission, its anti-Rayleigh fading ability is not high [7].

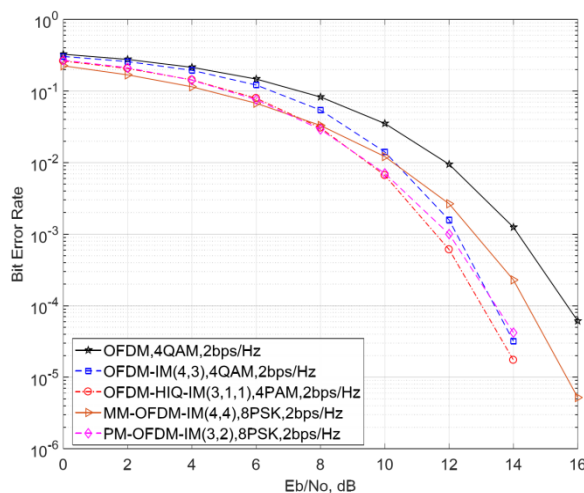


**Fig. 3** Enhancing Subcarrier Utilization in OFDM-IM Systems: A Comparative Analysis

Starting from improving the subcarrier utilization of OFDM-IM system, this chapter proposes an optimized index modulation scheme PM-OFDM-IM. As shown in Figure 3. The system model, subcarrier utilization and implementation scheme are analyzed specifically, and the complexity of ML detector and LLR detection is compared. The performance analysis of the proposed PM-OFDM-IM was carried out from three aspects, including the upper boundary of bit error rate, frequency offset resistance and reachable rate. From the analysis results, it is concluded that the upper bound of PM

OFDM-IM bit error rate is related to the channel conditions and the mapping constellation diagram, and PM-OFDM-IM has good resistance to frequency offset. From the simulation results, it can be concluded that PM-OFDM-IM improves the utilization rate of subcarriers while maintaining the advantages of index modulation system. These include gain in BER performance in Gaussian and Rayleigh channels and strong frequency offset immunity. From the conclusion of the upper bound and achievable rate of the bit error rate, it is found that in order to improve the system performance of PM-OFDM-IM, the key is to design a better constellation diagram. On the other hand, the PM-OFDM-IM system uses ML detectors to generate exponential complexity. The receiver should design a corresponding detector to reduce the complexity of ML detection.

## 4. Hybrid mapping scenarios

### 4.1. The Principle of Hybrid Mapping

In the traditional OFDM-IM mapping scheme, index mapping and The constellation symbol maps are independent of each other, with the index bits of each subcarrier group, the number is fixed at  $p_0$ , corresponding to the  $2^{p_0}$  type of SAP. For arbitrary sums  $n$  and  $k$ , in most cases there is  $w=C_n^k > 2^{p_0}$ , hence the traditional index mapping scheme is selected  $2p_0$  from the SAP to use, and the rest  $z=w-2p_0$  of SAP is disabled. According to  $2p_0 < w < 2p_0+1$ , we can know that  $w - 2z = w - 2(w - 2p_0) = 2p_0+1 - w > 0$ . This article mentions hybrid mapping scheme out will use all kinds of SAP, the former  $2z$  kinds of SAP which corresponds to the index bit sequence  $C_{\alpha}^*$  with length of  $(p_0+1)$ . In order to facilitate the unified processing of data symbols by the transmitter and receiver, let the  $C_{\alpha,1}^*$  with length of  $(p_1-1)$  do the perform parity, and complete the sequence of data bits of length  $p_1$ . It can be seen that the mapping methods corresponding to the first  $2z$  SAP of the hybrid mapping scheme are different from the traditional index mapping scheme, while the mapping methods of the last  $(w-2z)$  SAP are consistent with the traditional index mapping scheme. To distinguish between these two types of SAP, this topic defines the first  $2z$  SAP as super SAP, and the rest as normal SAP [8].

### 4.2. Performance Analysis

#### 4.2.1 Average False Bit Rate

The OFDM-IM system transmits and receives signals in units of subcarrier groups, so the BER performance of the system as a whole is equivalent to the BER performance of a subcarrier group [6]. This section uses the first subcarrier group as an example, and the conditional pairwise error probability of sending a sequence of symbols can be expressed as

$$P(X_1 \rightarrow \hat{X}_1 | H_1) = Q\left(\sqrt{\frac{\delta}{2N_F}}\right) \quad (11)$$

It can be approximated as

$$P(X_1 \rightarrow \hat{X}_1) = E_{H_1} \left\{ \frac{1}{12} e^{-q_1 \delta} + \frac{1}{4} e^{-q_2 \delta} \right\} \quad (12)$$

Average Bit Error Probability can be approximated as

$$P_b = \frac{1}{p_2^p} \sum_{X_1} \sum_{\hat{X}_1} P(X_1 \rightarrow \hat{X}_1) e(X_1 \rightarrow \hat{X}_1) \quad (13)$$

#### 4.2.2 Simulation Results and Analysis:

In order to verify the effectiveness of the hybrid mapping scheme proposed in this paper, MATLAB software is used to simulate the BER performance of the combined number method, the Gray code index mapping scheme and the mixed mapping scheme proposed in this paper [9]. Set the simulation parameters for all schemes as follows: number of subcarriers, channel is multipath fading channel, number of multipath, CP length is set to 16, and the modulation mode of data symbols is binary phase shift keying. The number of simulated frames is not less than 106, assuming that the

receiver is perfectly synchronized, and the channel estimation is error-free. Ignoring the effect of CP, let the energy per bit be  $E_b = m/N$ . As shown in Figure 4. The ABEP calculated from the theoretical value representation in the figure can be used as a mix combined with the theoretical BER value of the OFDM-IM system, ML means that the receiving end adopts maximum likelihood detection, and LLR indicates that the receiving end adopts LLR detection. Figures below represents the combination number method, Gray code represents the gray code index mapping scheme, hybrid represents the hybrid mapping scheme, and the receiving end of the OFDM-IM system of the three schemes all use ML detection algorithm [10].

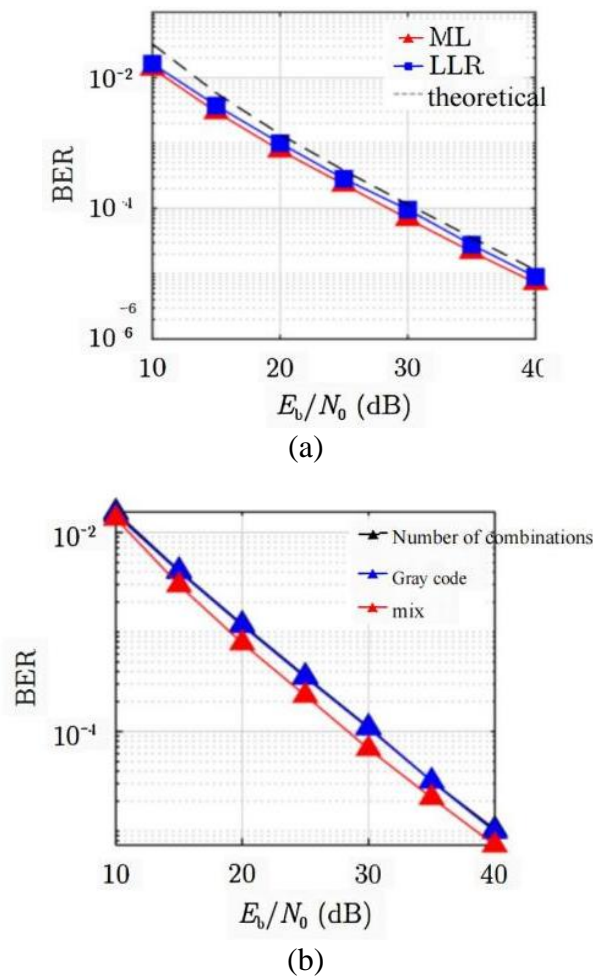


**Fig. 4** Comparative Analysis of Gray Code and Hybrid Mapping Schemes in OFDM-IM Systems using ML Detection Algorithm

## 5. Conclusion

In an effort to further enhance the bit error performance of index-modulated OFDM systems under high signal-to-noise ratios, we propose a hybrid mapping scheme. This method leverages the lower bit-error rate of indexed bit-ratio data in high signal-to-noise environments, merging two distinct bit-allocation strategies and increasing the proportion of index bits. To reduce the complexity of Maximum Likelihood (ML) detection at the receiver end, we've designed a low-complexity Log-Likelihood Ratio (LLR) detection algorithm for this hybrid model. We've analyzed the Bit Error Rate (BER) performance of this approach using pairwise error probability theory, comparing it with the combinatorial number method and the gray code index mapping scheme. We also derive the system's average bit error rate. In comparison with the combinatorial number method and the gray code index mapping scheme, when the index bit mapping is super SAP, our hybrid mapping approach not only enhances the system's diversity but also increases the minimum Euclidean distance between data

symbols, effectively boosting the system's BER performance. The effectiveness of our proposed method is verified through MATLAB software simulations. We analyzed the factors influencing the BER performance gain of our scheme, finding a performance gain of 1~3 dB during BPSK/QPSK modulation with our proposed hybrid mapping scheme. OFDM technology's emergence aligns with today's societal demand for high-speed data transmission. Its unique anti-interference capability and improved spectrum utilization have drawn global attention. The fusion of OFDM with other technologies effectively addresses the limitations inherent in standalone techniques, boosts the throughput of MIMO data transmission systems, and solves the problem of efficient digital video broadcasting in challenging ground conditions. Its application extends to vehicular broadcasting and wireless local area networks, significantly increasing network throughput, enabling high-speed information transmission while ensuring compatibility.

## References

- [1] Wang, Y., Jiang, B., & Liu, J. (2019). A survey of multimodal emotion recognition research. *Information Fusion*, 52, 222-237.
- [2] Baltrusaitis, T., Robinson, P., & Morency, L. P. (2018). Multimodal emotion analysis in the wild. *Image and Vision Computing*, 68, 101-115.
- [3] Karray, F., & Saleh, J. A. (2018). Multimodal Emotion Recognition Using Deep Neural Networks: A Review. *IEEE Transactions on Affective Computing*, 9(3), 377-401.
- [4] Song, X., Lu, D., & Li, H. (2020). Multimodal Emotion Recognition Based on Deep Learning: A Survey. *IEEE Transactions on Cognitive and Developmental Systems*, 12(3), 567-579.
- [5] Yin, M., Duan, J., Zhang, Y., Zhang, S., & Yan, Q. (2019). Multimodal emotion recognition based on deep neural network. *IEEE Access*, 7, 7093-7103.
- [6] Li, Y., Mao, Y., Chen, L., & Lin, C. Y. (2018). A survey of multimodal emotion recognition using physiological signals. *Information Fusion*, 45, 99-113.
- [7] Zhao, Y., Wu, X., Wang, L., Zhang, J., & Chen, Y. (2020). A Survey on Multimodal Emotion Recognition Methods and Applications. *Frontiers in Psychology*, 11, 335.
- [8] Guan, J., Wang, D., & Hong, X. (2017). Multimodal emotion recognition using dynamic fuzzy support vector machine. *IEEE Transactions on Cybernetics*, 48(5), 1393-1404.
- [9] Liu, Y., Wang, Y., & Zhang, J. (2019). Convolutional neural network based multimodal emotion recognition applied to video game.
- [10] Wang, S., Li, Y., & Li, Q. (2017). Multimodal emotion recognition using sparse autoencoder neural network. *IEEE Transactions on Industrial Electronics*, 64(8), 6486-6495.